Marigold Flower-Like Assemblies of Phosphorescent Iridium-Silver Coordination Polymers

*Diego Rota Martir,[a] Pachaiyappan Rajamalli,[a] David B. Cordes,[a] Alexandra M. Z. Slawin,[a] and Eli Zysman-Colman[a]**

[a]Organic Semiconductor Centre, EaStCHEM School of Chemistry, University of St Andrews, St Andrews, Fife, KY16 9ST, UK, Fax: +44-1334 463808; Tel: +44-1334 463826; E-mail: eli.zysman-colman@st-andrews.ac.uk;
URL: http://www.zysman-colman.com

Abstract. Racemic and enantiopure phosphorescent iridium(III)-silver(I) coordination polymers are reported. The polymers *rac*-, Λ- and Δ-**IrAg** were formed, respectively, by the assembly of the chiral iridium metalloligands *rac*-, Λ- and Δ-[Ir(mesppy)$_2$(qpy)]PF$_6$ (*rac*-, Λ- and Δ-**Ir**) where mesppy is 2-phenyl-4-mesitylpyridinato and qpy is 4,4':2',2'':4'',4'''-quaterpyridine, and Ag^+ ions through N_{py}-Ag linear coordination. The polymers have been characterized in $MeNO_2$ solution by ^{1}H and ^{1}H DOSY NMR and CD spectroscopies and in the solid-state by Scanning Electron Microscopy (SEM); the crystal structures of the racemic polymer *rac*- **IrAg** has been obtained by X-ray diffraction. The polymers *rac*-, Λ- and Δ-**IrAg** exhibited orange/red emission in solution, in films and as crystals, with intensities comparable to those of the corresponding iridium metalloligands *rac*-, Λ- and Δ-**Ir**. The morphology of the enantiopure polymers in the solid-state resemble marigold flower-like nano-porous assemblies while the racemic polymer possesses an irregular morphology formation.

Introduction. Crystal engineering is a powerful approach to self-organize ligand molecules and metal ions in the solid-state into infinite 1D-, 2D- and 3D- metal-organic supramolecular materials through non-covalent interactions.[1] In recent years, an increased understanding of

the main factors controlling the self-assembly of simple metal-organic architectures has been gained; appropriate matching of the coordination geometry preferences of metal ion(s), the nature and denticity of the ligand scaffold, and the length, angle and flexibility of the linking units between binding sites on the ligands generally provide good control on the resulting assembly.[1a, 2]

The coordination sphere of Ag^+ ions is particularly flexible and Ag^+ can adopt a coordination number between one and six, corresponding to the coordination geometries of linear,[3] trigonal,[4] tetrahedral,[5] square planar,[6] square pyramidal,[7] trigonal bipyramidal[8] and octahedral.[9] This geometric flexibility thus gives rise to intricate coordination structures, the self-assembly process of which is generally influenced by the modification of the ligand functionalities, anions, solvents, ligand-to-Ag ratio, as well as crystallisation conditions.[10] The nature of the Ag(I)-N_{py} interaction is predominantly donation of the pyridine electron lone pair to the metal cation and its energy is comparable with that of a strong H-bond (for example, 47 $kJ \cdot mol^{-1}$ for Ag(I)-pyridine).[11] Ag(I)-N_{py} bonding has been exploited quite extensively to form linear and zig-zag and helical supramolecular chains.[11-12] Linear structures can be easily formed by the assembly a ligand containing two pyridine units disposed in a linear arrangement with Ag^+ ions in a 1:1 stoichiometry.[13] On the other hand, if bent ditopic ligands are assembled with Ag(I) or if the linear Ag(I) coordination geometry is distorted by coordinating anions or solvents, zig-zag chains or polymeric helical motifs are likely to be formed.[12c, 14] Both linear and zigzag chains can further assemble into a network or a macrocycle in the presence of a connecting entity such as solvent molecules or anions.

Herein we report chiral phosphorescent coordination polymers, *rac*-, Λ- and Δ-**IrAg**, formed respectively through the self-assembly between the iridium metalloligand *rac*-, Λ- and Δ-**Ir** of composition *rac*-, Λ- and Δ-[Ir(mesppy)$_2$(qpy)]PF_6 (Figure **1**) and Ag^+ ions through N_{py}-Ag linear coordination. Although in recent years the use of iridium(III) complexes as luminescent components in 3D-assemblies such as Metal-Organic Frameworks (MOFs) and Coordination Polymers (CP) has become increasingly popular,[15] to the best of our knowledge, these are the first examples of coordination polymers formed through the assembly between an iridium metalloligand and silver ions. Phosphorescent silver(I) coordination polymers themselves are rare and limited to silver-triazolates,[16] such as those found by Zhou and co-workers,[16a, 16b] consisting of cyanide-containing Ag^+ polymers that exhibit broad green emissions located at λ_{PL} between 500 and 520 nm. The emission from triplet states in these coordination polymers is induced by the heavy atom effect of silver(I) ions and is ascribed to a mixture of an ^{3}MLCT transition, where electron is transferred from Ag(I) centre to π* orbitals of the triazolates, and an ^{3}LLCT, cyanide-to-triazole charge transfer transition. 3D heterometallic coordination polymers and MOFs containing Ag(I) nodes were also reported by the groups of Englert,[17] Hosseini,[18] Mahon,[19] Severin,[20] Cohen[21] and Carlucci[22] by reacting tritopic octahedral Fe(III), Al(III), Co(III), Cr(III), In(III) and Ga(III) metalloligands or ditopic tetrahedral Zn(II), Cu(II) and Pd(II) metalloligands, all containing 3-cyano acetylacetonato units, with Ag^+ metal ions. These 3D heterometallic assemblies were found to be either non-emissive or no comment is made on their emission properties.

Results and discussion

The self-assembly between the metalloligands *rac*-, Λ- and Δ-**Ir** (Figure **1**), previously reported by us to form phosphorescent $[Pd_4Ir_8]^{16+}$ coordination cages in the presence of Pd^{2+} ions,[23] and $AgPF_6$ was first investigated at room temperature by ^{1}H and ^{1}H-DOSY NMR

spectroscopy in $MeNO_2$-d_3, a solvent chosen to not interfere with the linear coordination of the distal pyridines present in the metalloligands with Ag^+ ions. When a 3.0 mM $MeNO_2$-d_3 solution of any of the metalloligands *rac*-, Λ- and Δ-**Ir** was mixed for five minutes with one equivalent of $AgPF_6$, the proton resonances associated with *rac*-, Λ- and Δ-**Ir** slightly broadened and were shifted (Figure **2a** and Figure **S1**,**2**). The broad ^{1}H NMR signals are indicative of the formation of large structures, the tumbling motion of which is slow on the NMR time scale.[24]

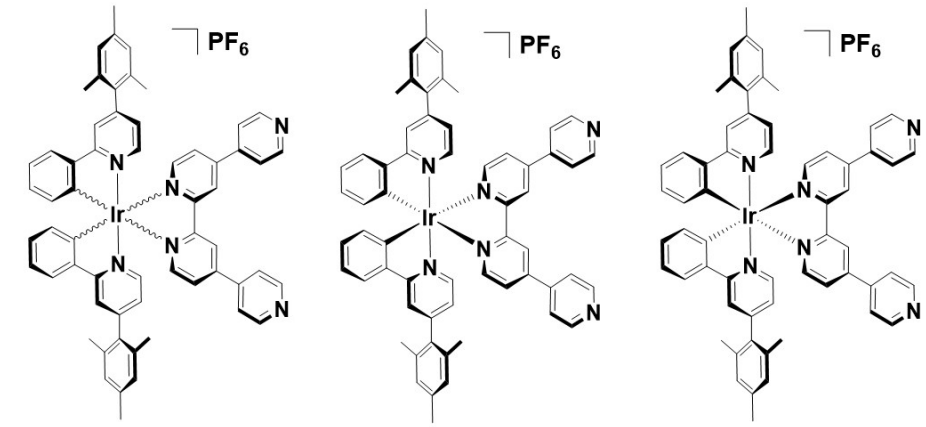

Figure **1**. Chemical structures of metalloligands *rac*-, Λ- and Δ-**Ir**.

For each metalloligand ^{1}H DOSY NMR spectra showed the formation of single and identical species in $MeNO_2$-d_3 solution with diffusion coefficients of $D = 2.84 \times 10^{-10}$, 2.87×10^{-10} and 2.86×10^{-10} m^2/s for *rac*-, Λ- and Δ-**Ir**, respectively. These diffusion coefficients are smaller than those measured for *rac*-, Λ- and Δ-**IrAg** in $MeNO_2$-d_3 ($D = 4.08 \times 10^{-10}$ m^2/s), indicating that the assembled structure, *rac*-, Λ- and Δ-**IrAg**, are larger than the corresponding metalloligand (Figure **2b** and Figure **S3**). The corresponding hydrodynamic radii (r_s) for *rac*-, Λ- and Δ-**IrAg** in $MeNO_2$-d_3 were calculated to each be 12.5 Å, which is approximately 50% larger than those calculated for *rac*-, Λ- and Δ-**Ir** (r_s = 8.6 Å). Therefore, *rac*-, Λ- and Δ-**IrAg**

in $MeNO_2$-d_3 solution are identical and comprises short **Ir**-Ag oligomers. The addition of a larger amount of $AgPF_6$ (2 or 5 equivalents) to the $MeNO_2$-d_3 solution of *rac*-, Λ- and Δ-**IrAg** did not cause any further changes to the ^1H and ^1H-DOSY NMR spectra of *rac*-, Λ- and Δ-**IrAg**, indicating the assembly in solution is formed with a 1:1 stoichiometry between the metalloligand and Ag^+.

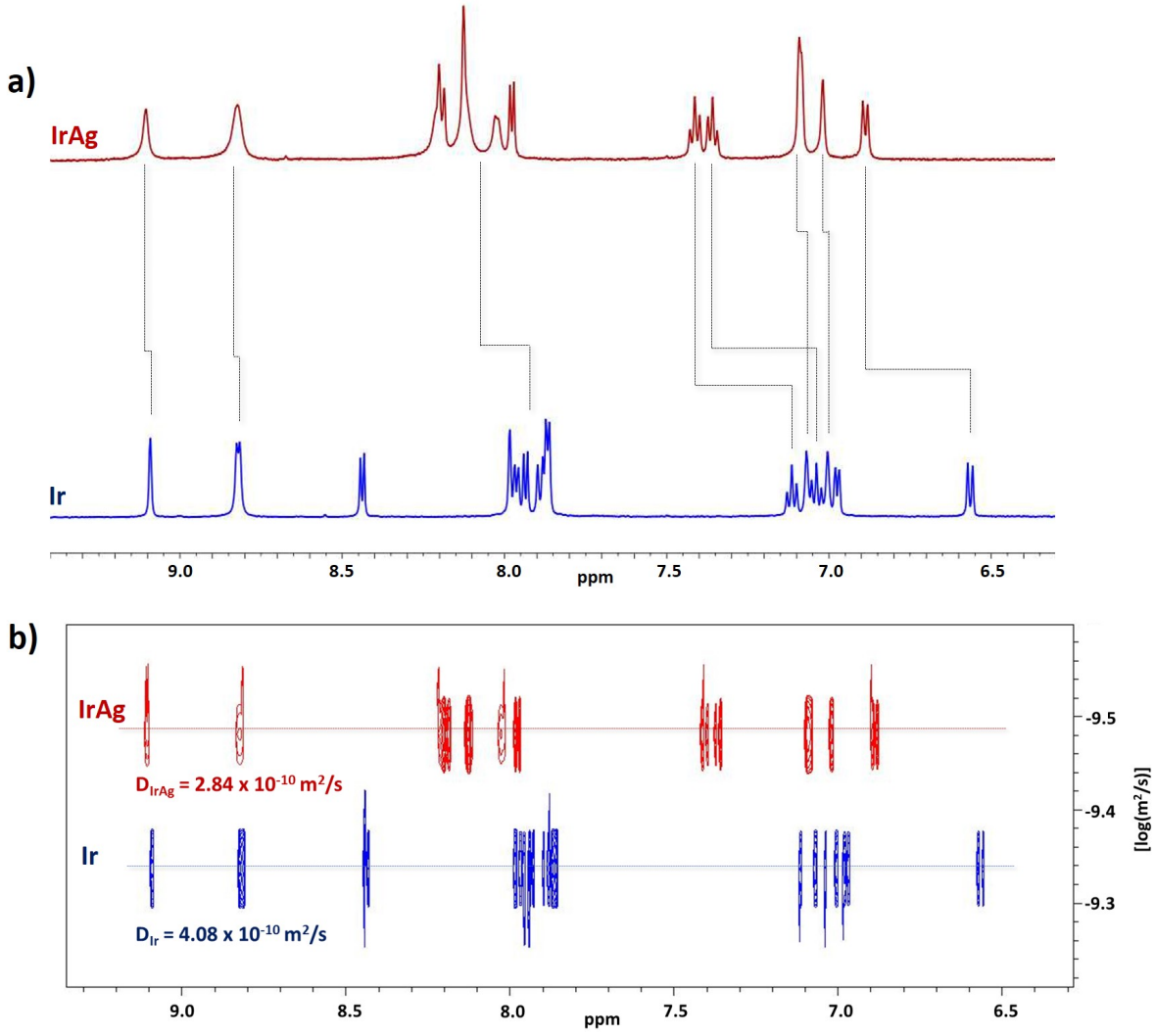

Figure **2**. **a)** ^1H NMR spectra of *rac*-**Ir** (in blue) and a 1:1 mixture of *rac*-**Ir**:$AgPF_6$ (*rac*-**IrAg**, in red); **b)** ^1H DOSY NMR spectra of *rac*-**Ir** (in blue) and a 1:1 mixture of *rac*-**Ir**:$AgPF_6$ (*rac*-**IrAg**, in red). The NMR spectra were collected in $MeNO_2$-d_3 at room temperature at a concentration of *rac*-**Ir** of 3.0 mM.

The CD spectra of Λ- and Δ-**IrAg** revealed that these were homochiral assemblies (Figure **3**) with mirror image spectra. As expected, when *rac*-**Ir** was employed as the metalloligand, a racemic polymer (*rac*-**IrAg**) was formed.

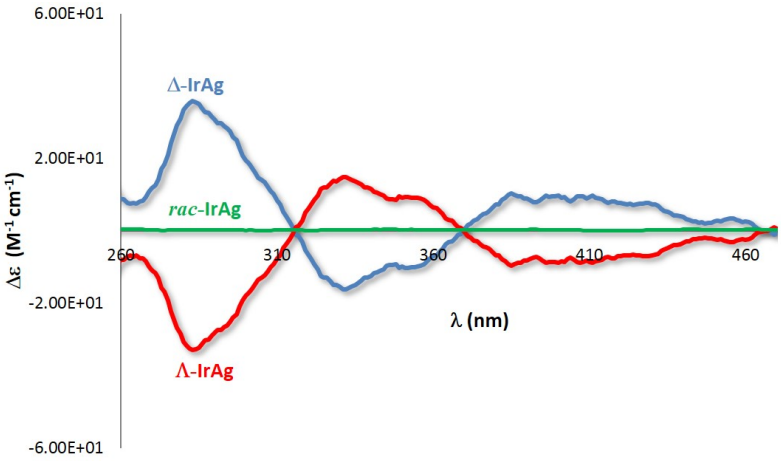

Figure **3**. CD spectra collected in CH_2Cl_2 at 298 K of *rac*-**IrAg** (green line); Λ-**IrAg** (blue line) and Δ-**IrAg** (red line). The CD spectra were collected at a concentration of 1×10^{-5} M.

Single crystals of *rac*-**IrAg** suitable for X-ray diffraction were obtained through a slow diffusion over 10 days of diethyl ether into a 3 mM DCM solution *rac*-**Ir** (1 mL) layered with a 1:1 DCM/MeOH mixture (1 mL) and then with a MeOH solution of $AgPF_6$ (1 mL). *rac*-**IrAg** crystallised in the triclinic space group $P\bar{1}$, with two independent Ag(I) ions situated on inversion centers, coordinating the two N_{qpy} atoms of one molecule of **Ir**. The inversion symmetry leads to a linear coordination geometry at Ag(I) and gives rise to a racemic, 1D zig-zag coordination polymer (Figure **4**) where every Ag(I) is coordinated by one Λ-**Ir** and one Δ-**Ir** enantiomer. The $N_{qpy}\cdots Ag\cdots N_{qpy}$ distances [2.141(19) and 2.156(19) Å] are similar to the range of $N_{py}\cdots Ag\cdots N_{py}$ distances (1.9 – 2.1 Å) reported for the X-ray structures of related silver(I) coordination polymers.[12a] However, in many of these literature structures the linear Ag(I)

coordination ($N_{py}\cdots Ag\cdots N_{py}$) is distorted by the presence of coordinating or weakly interacting anions (PF_6^-, BF_4^-, AsF_6^- or ClO_4^-) or solvent molecules.[10, 25] This is not the case for *rac*-**IrAg**. Indeed, for *rac*-**IrAg**, despite the presence in the crystal lattice of weakly coordinating PF_6^- anions, the Ag(I) centres coordinate to the N_{qpy} atoms with a perfect symmetry-induced linear geometry without any interaction with the fluorine atoms of PF_6^-.

The packing of the 1D chains of *rac*-**IrAg** shows weak hydrogen bonds between the fluorine atoms of the PF_6^- counterions and C–H hydrogen atoms of several pyridine rings of the mesppy moieties of the metalloligand [C–H···F–PF_5^- distances of 2.36 – 2.50 Å, with corresponding C···F separations of 3.13(2) – 3.35(5) Å]. This gives rise to weakly hydrogen-bonded layers in the *ab*-plane. However, *rac*-**IrAg** does not show any direct chain-to-chain intermolecular interactions, such as π-π stacking, likely due to the presence of the bulky mesityl substituents. The Ir···Ir separations between two adjacent metalloligands connected by the Ag(I) bridge is 22.409(3) Å while the Ir···Ir distance between two iridium complexes located in parallel 1D chains mediated by PF_6^- counterions is less than half of this, at 10.8838(18) Å. However, shorter Ir···Ir distances are found between Ir centers in adjacent sheets, at 8.806(16) Å. *rac*-**IrAg** packs to form a complex three-dimensional network of narrow pores, giving a total free space of approximately 1285 $Å^3$ (~33 % of the volume of the unit cell).

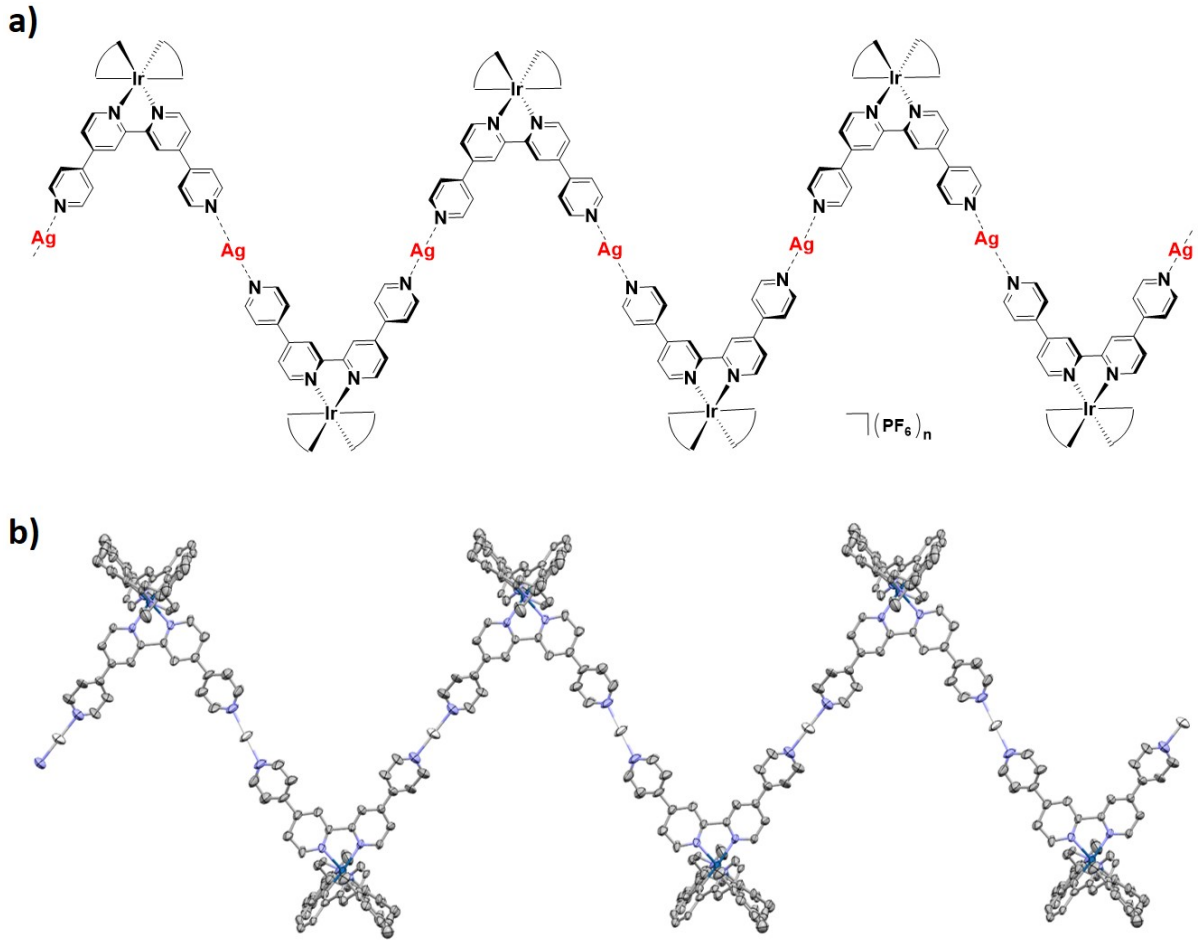

Figure **4**. **a)** Representation of the structure of the zig-zag coordination polymer *rac*-**IrAg**. The mesppy C^N ligands have been omitted for clarity; **b)** View of the X-ray structure of one 1D chain of *rac*-**IrAg**. Hydrogen atoms, solvent molecules and counterions have been omitted for clarity.

Although apparently single crystals of the enantiopure polymers Λ- and Δ-**IrAg** could also be grown following the same crystallisation condition used for *rac*-**IrAg**, and were examined by X-ray diffraction, their diffraction was too weak and was not being amenable to refinement. We then turned our attention to investigate the morphologies of the crystals of Λ- and Δ-**IrAg** by SEM. The crystals were grown on a silicon surface through a slow diffusion of diethyl ether into 3 mM DCM solutions of Λ- and Δ-**Ir** (1 mL) layered with a 1:1 DCM/MeOH mixture (1 mL) and then with a MeOH solution of $AgPF_6$ (1 mL). Interestingly, the SEM images show

that Λ- and Δ-**IrAg** are assembled in the solid-state into porous nanospheres with diameters ranging from 20 and 40 μm and with shapes reminiscent of marigold flowers (Figure **4** and Figure **S6**,**7**).

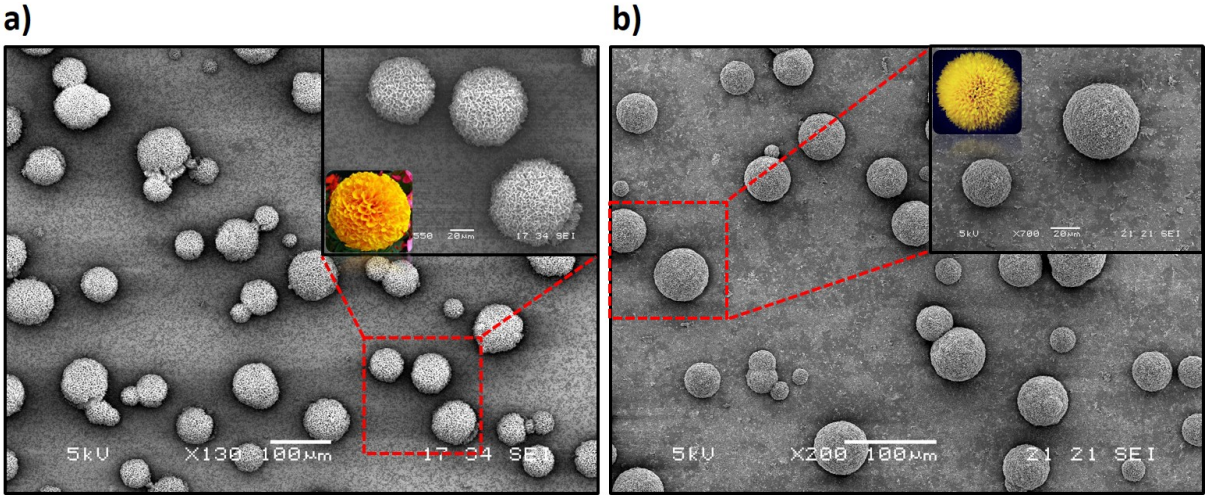

Figure **5**. **a)** SEM images of the crystals of Δ-**IrAg** and **b)** SEM images of the crystals of Λ-**IrAg**. Insets are zoomed images of the nanospheres with representations of Marigold flowers.

The porous and spherical morphology exhibited in the solid-state by Λ- and Δ-**IrAg** is often observed for inorganic nanostructures[26] such as metal oxide nanoparticles,[27] gold[28] and silicon nanoparticles,[29] but it is very rare for metal-based coordination polymers.[30] On the other hand, the crystals of *rac*-**IrAg**, which require the presence in the lattice of both the Λ and Δ enantiomers to form the polymer chain illustrated in Figure **4b**, exhibit a different morphology compared to that of the crystals of Λ- and Δ-**IrAg**. SEM analysis revealed that *rac*-**IrAg** forms a flake-shaped nanostructure and square shaped crystals (Figure **S5**). Therefore, the chirality of the metalloligand *rac*-, Λ- and Δ-**Ir** plays a key role in the resulting morphology of the polymer assemblies in the solid-state.

Emission properties

The emission properties of the *rac*-, Λ- and Δ-**Ir** metalloligands and *rac*-, Λ- and Δ-**IrAg** coordination polymers were investigated in deaerated $MeNO_2$, as crystals and in thin films (Table **1**). In deaerated $MeNO_2$, all three metalloligands exhibit an emission centered at λ_{PL} = 614 nm, with identical photoluminescence quantum yields, Φ_{PL}, of 12% and similar photoluminescence lifetimes, $\tau_{PL,}$ of 284, 290 and 297 ns, respectively. These emission properties match with those seen in deaerated DCM.[23] The emissions of the coordination polymers *rac*-, Λ- and Δ-**IrAg** in deaerated $MeNO_2$ are all slightly broader and red-shifted at 646 nm, with slightly higher Φ_{PL} of 15%, 14% and 15% and slightly longer τ_{PL} of 375, 382 and 379 ns compared to the corresponding metalloligand (Figure **5** and Figure **S8**). The red-shifted emission of *rac*-, Λ- and Δ-**IrAg** compared to *rac*-, Λ- and Δ-**Ir** is the result of the coordination of the metalloligands to the Lewis-acidic Ag(I), which stabilizes the metalloligand-centred LUMO of in *rac*-, Λ- and Δ-**IrAg**, resulting in a smaller HOMO-LUMO gap and a correspondingly stabilized triplet excited state. The radiative rate constant, k_r, calculated for *rac*-, Λ- and Δ-**IrAg** of 4.0×10^5 s^{-1} is similar to that of *rac*-, Λ- and Δ-**Ir** while its non-radiative rate constant, k_{nr}, of 2.3×10^6 s^{-1} is slightly lower (for *rac*-, Λ- and Δ-**Ir** $k_r = 4.2 \times 10^5$ s^{-1}, $k_{nr} = 3.9 \times 10^6$ s^{-1}), which we attributed to a rigidification of the iridium luminophores assembled into organized chains. Thus, the silver ions do not adversely affect the emission properties of **IrAg** in $MeNO_2$, where, as evidenced by ^{1}H DOSY NMR measurements, short coordination oligomers are present. The emissions exhibited by the crystals of *rac*-, Λ- and Δ-**IrAg**, respectively, at 665, 661 and 664 nm (Figure **6a** and **S9**) are red-shifted compared to those collected in $MeNO_2$ solution, with lower Φ_{PL} of 4.6%, 9.2% and 8.9% and shorter biexponential τ_{PL} of 63, 181 ns and 79, 192 ns and 83, 208 ns (Table **1**). It is interesting to note that the irregular flake-shaped nanostructures and square shaped crystals of *rac*-**IrAg** exhibited lower Φ_{PL} compared to those exhibited by the porous nanospheres of Λ- and Δ-**IrAg**, which

showed almost identical emission properties. The lower Φ_{PL} of *rac*-**IrAg** was attributed to the formation of irregular and compact morphologies, which promote stronger intermolecular interactions between the iridium complexes with the concomitant enhancement of their emission quenching. The emissive nature of *rac*-, Λ- and Δ-**IrAg** both in solution and as crystals contrast with the behavior reported by Hosseini and co-workers for an Ir-Cu coordination network,[31] which was found to be non-emissive both in solution and in the crystalline state, indicating that the Cu^{+} metal ions completely quenched the luminescence of the Ir metalloligand $[Ir(ppy)_2(py\text{-}bpy)]PF_6$ (ppy is 2-phenylpyridinato and py-bpy is 5,5'-bis(pyridin-4-ylethynyl)-2,2'-bipyridine), which itself exhibited a Φ_{PL} of 19% in deaerated THF and of 2% in the solid state. The Ir-Cd network, reported by the same group,[32] exhibited a weak emission (Φ_{PL} of 1%) in the crystalline state, which was, as observed for *rac*-, Λ- and Δ-**IrAg**, slightly red-shifted ($\Delta\lambda = 6.67 \times 10^5$ cm^{-1}, 15 nm) and of similar intensity when compared to the solid-state emission of the corresponding Ir metalloligand Δ-, *rac*-$[Ir(ppy)_2(py\text{-}bpy)]PF_6$. In neat film the emissions of *rac*-, Λ- and Δ-**IrAg** was broader and blue-shifted, respectively, at 592, 592 and 598 nm with slightly reduced Φ_{PL} of 3.9%, 3.4% and 3.6% and shorter bi-exponential τ_{PL} of 32, 142 ns; 42, 165 ns and 41, 161 ns (Figures **S10-S16**).

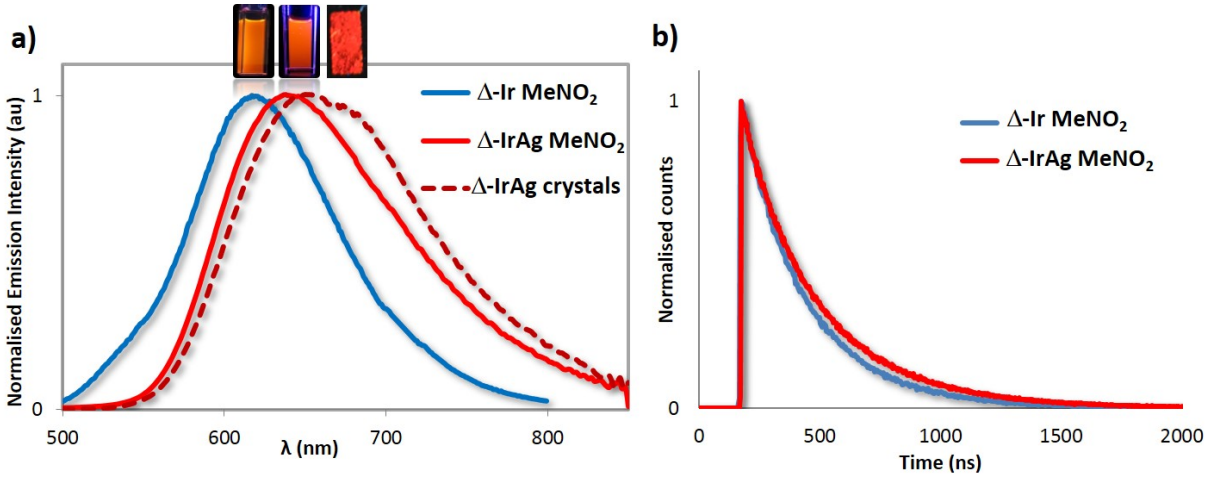

Figure **6**. **a)** emission spectra of Δ-**Ir** (solid blue line) and Δ-**IrAg** (solid red line) in deaerated $MeNO_2$ and of crystals of Δ-**IrAg** (dotted red line) collected at 298 K, λ_{exc} = 360 nm and **b)** emission lifetimes of Δ-**Ir** (blue line) and Δ-**IrAg** (red line), λ_{exc} = 378 nm collected in deaerated $MeNO_2$ at 298 K.

Table **1**. Photophysical properties of ***rac*-, Λ- and Δ-Ir and *rac*-, Λ- and Δ-IrAg**.

	λ_{em} / nm			Φ_{PL} / %			τ_{PL} / ns		
	DCM[a]	Crystals	Film[b]	DCM[c]	Crystals[c]	Film[b,d]	DCM[a]	Crystals	Film[b,e]
***rac*-Ir**	614	-	621	12	-	7.6	284	-	241 (0.77), 591 (0.23)
Δ-Ir	614	-	620	12	-	7.1	290	-	160 (0.73), 474 (0.27)
Λ-Ir	614	-	619	12	-	6.9	297	-	183 (0.80), 436 (0.20)
***rac*-IrAg**	646	665	592	15	4.6	3.9	375	63 (0.53), 181 (0.47)	32 (0.52), 142 (0.48)
Δ-IrAg	646	661	592	14	9.2	3.4	382	79 (0.40), 192 (0.60)	42 (0.56), 175 (0.44)
Λ-IrAg	646	664	598	15	8.9	3.6	379	83 (0.52), 208 (0.48)	41 (0.59), 161 (0.41)

[a] Measurements in degassed $MeNO_2$ at 298 K (λ_{exc} = 360 nm). [b] Thin films formed by spin-coating on a pristine quartz substrate. [c] Φ_{PL} measurements were carried out in degassed $MeNO_2$ under nitrogen (λ_{exc} = 360 nm) using quinine sulfate as the external reference (Φ_{PL} = 54.6% in 0.5 M H_2SO_4 at 298 K).[33] [d] Values obtained using an integrating sphere. [e] Values in parentheses are pre-exponential weighting factor, in relative % intensity, of the emission decay kinetics (λ_{exc} = 378 nm).

Conclusions

We have herein reported the first examples of phosphorescent coordination polymers formed through the self-assembly between the iridium complexes *rac*-, Λ- and Δ-

[Ir(mesppy)$_2$(qpy)]PF$_6$ and Ag^+ metal ions through N_{qpy}-Ag coordination. The structure of the racemic *rac*-**IrAg**, elucidated by X-ray crystallography, shows a zigzag coordination polymer formed by through linear coordination of Ag(I) metal centres with the ditopic qpy moiety of the iridium metalloligand. In the solid-state, *rac*-**IrAg** assembles into nanostructures of irregular morphologies while enantiopure Λ- and Δ-**IrAg** form porous nanospheres resembling the shape of marigold flowers. The silver metal ions promoted a red-shift in the emission of the coordination polymers both in $MeNO_2$ and as crystals but do not adversely influence the photoluminescence quantum yields and lifetimes. We therefore believe that the assembly of suitably functionalised phosphorescent metal complexes with Ag^+ ions as structural components opens up the possibility to prepare a wide range of supramolecular architectures such as coordination polymers, networks and macrocycles, that retain the optoelectronic properties of the photoactive complexes.

Supplementary materials

Experimental section, characterization of iridium complexes and coordination polymers, crystal structure of *rac*-**IrAg**, Scanning Electron Microscopy measurements and supplementary optoelectronic data.

Acknowledgements

EZ-C acknowledges the University of St Andrews and EPSRC (EP/M02105X/1) for financial support. We thank the EPSRC UK National Mass Spectrometry Facility at Swansea University for analytical services. We thank Umicore AG for the gift of materials.

References

[1] a) R. Chakrabarty, P. S. Mukherjee, P. J. Stang, *Chem. Rev.* **2011**, *111*, 6810; b) L. Chen, Q. Chen, M. Wu, F. Jiang, M. Hong, *Acc. Chem. Res.* **2015**, *48*, 201.

[2] M. M. J. Smulders, I. A. Riddell, C. Browne, J. R. Nitschke, *Chem. Soc. Rev.* **2013**, *42*, 1728.

[3] C.-Y. Su, Y.-P. Cai, C.-L. Chen, M. D. Smith, W. Kaim, H.-C. zur Loye, *J. Am. Chem. Soc.* **2003**, *125*, 8595.

[4] D. Sun, R. Cao, W. Bi, X. Li, Y. Wang, M. Hong, *Eur. J. Inorg. Chem.* **2004**, *2004*, 2144.

[5] Y.-B. Dong, X. Zhao, R.-Q. Huang, M. D. Smith, H.-C. zur Loye, *Inorg. Chem.* **2004**, *43*, 5603.

[6] a) A. G. Young, L. R. Hanton, *Coord. Chem. Rev.* **2008**, *252*, 1346; b) S. Chowdhury, M. G. B. Drew, D. Datta, *New J. Chem.* **2003**, *27*, 831.

[7] C.-L. Chen, C.-Y. Su, Y.-P. Cai, H.-X. Zhang, A.-W. Xu, B.-S. Kang, H.-C. zur Loye, *Inorg. Chem.* **2003**, *42*, 3738.

[8] A. Kyono, M. Kimata, T. Hatta, *Inorg. Chim. Acta* **2004**, *357*, 2519.

[9] C. Lucia, C. Gianfranco, P. Francesca, P. D. M., S. Laura, *Angew. Chem. Int. Ed.* **2002**, *41*, 1907.

[10] F. Zhang, S. A. Baudron, M. W. Hosseini, *CrystEngComm* **2017**, *19*, 4393.

[11] A. N. Khlobystov, A. J. Blake, N. R. Champness, D. A. Lemenovskii, A. G. Majouga, N. V. Zyk, M. Schröder, *Coord. Chem. Rev.* **2001**, *222*, 155.

[12] a) C.-L. Chen, B.-S. Kang, C.-Y. Su, *Aust. J. Chem.* **2006**, *59*, 3; b) P. Rajamalli, P. Malakar, S. Atta, E. Prasad, *Chem. Commun.* **2014**, *50*, 11023; c) L. Carlucci, G. Ciani, D. M. Proserpio, A. Sironi, *Inorg. Chem.* **1998**, *37*, 5941.

[13] G. K. Patra, I. Goldberg, *Crystal Growth & Design* **2003**, *3*, 321.

[14] M. Maekawa, H. Konaka, Y. Suenaga, T. Kuroda-Sowa, M. Munakata, *J. Chem. Soc., Dalton Trans.* **2000**, *22*, 4160.

[15] D. Rota Martir, E. Zysman-Colman, *Coord. Chem. Rev.* **2018**, *364*, 86.

[16] a) Y. Ling, F.-P. Zhai, M.-L. Deng, D. Wu, Z.-X. Chen, X.-F. Liu, Y.-M. Zhou, L.-H. Weng, *CrystEngComm* **2012**, *14*, 1425; b) Y. Ling, Z.-X. Chen, Y.-M. Zhou, L.-H. Weng, D.-Y. Zhao, *CrystEngComm* **2011**, *13*, 1504; c) Q.-G. Zhai, M.-C. Hu, S.-N. Li, Y.-C. Jiang, *Inorg. Chim. Acta* **2009**, *362*, 1355.

[17] a) A. Wang, C. Merkens, U. Englert, *CrystEngComm* **2015**, *17*, 4293; b) C. Merkens, N. Becker, K. Lamberts, U. Englert, *Dalton Trans* **2012**, *41*, 8594.

[18] a) B. Kilduff, D. Pogozhev, S. A. Baudron, M. W. Hosseini, *Inorg Chem* **2010**, *49*, 11231; b) D. Pogozhev, S. A. Baudron, M. W. Hosseini, *Inorg Chem* **2010**, *49*, 331.

[19] A. D. Burrows, K. Cassar, M. F. Mahon, J. E. Warren, *Dalton Trans* **2007**, 24 , 2499.

[20] M. Marmier, G. Cecot, A. V. Vologzhanina, J. L. Bila, I. Zivkovic, H. M. Ronnow, B. Nafradi, E. Solari, P. Pattison, R. Scopelliti, K. Severin, *Dalton Trans* **2016**, *45*, 15507.

[21] J. R. Stork, V. S. Thoi, S. M. Cohen, *Inorg. Chem.* **2007**, *46*, 11213.

[22] L. Carlucci, G. Ciani, S. Maggini, D. M. Proserpio, M. Visconti, *Chemistry* **2010**, *16*, 12328.

[23] D. Rota Martir, D. Escudero, D. Jacquemin, D. B. Cordes, A. M. Z. Slawin, H. A. Fruchtl, S. L. Warriner, E. Zysman-Colman, *Chem. Eur. J.* **2017**, *23*, 14358.

[24] a) D. Rota Martir, D. B. Cordes, A. M. Z. Slawin, D. Escudero, D. Jacquemin, S. L. Warriner, E. Zysman-Colman, *Chem. Commun.* **2018**, *54*, 6016; b) D. R. Martir, A.

Pizzolante, D. Escudero, D. Jacquemin, S. L. Warriner, E. Zysman-Colman, *ACS Applied Energy Materials* **2018**, *1*, 2971.
[25] A. Mazel, S. A. Baudron, M. W. Hosseini, *CrystEngComm* **2017**, *19*, 897.
[26] J. Liu, T. Yang, D.-W. Wang, G. Q. Lu, D. Zhao, S. Z. Qiao, *Nature Communications* **2013**, *4*, 2798.
[27] a) M. Cargnello, D. Sala, C. Chen, M. D'Arienzo, R. J. Gorte, C. B. Murray, *RSC Advances* **2015**, *5*, 41920; b) B. Liu, K. Nakata, M. Sakai, H. Saito, T. Ochiai, T. Murakami, K. Takagi, A. Fujishima, *Catalysis Science & Technology* **2012**, *2*, 1933.
[28] Q. Zhang, N. Large, P. Nordlander, H. Wang, *J Phys Chem Lett* **2014**, *5*, 370.
[29] D. Cassano, D. Rota Martir, G. Signore, V. Piazza, V. Voliani, *Chem. Commun.* **2015**, *51*, 9939.
[30] a) A. M. Spokoyny, D. Kim, A. Sumrein, C. A. Mirkin, *Chem. Soc. Rev.* **2009**, *38*, 1218; b) A. Umemura, S. Diring, S. Furukawa, H. Uehara, T. Tsuruoka, S. Kitagawa, *J. Am. Chem. Soc.* **2011**, *133*, 15506.
[31] C. Xu, A. Guenet, N. Kyritsakas, J.-M. Planeix, M. W. Hosseini, *Chem. Commun.* **2015**, *51*, 14785.
[32] C. Xu, A. Guenet, N. Kyritsakas, J.-M. Planeix, M. W. Hosseini, *Inorg. Chem.* **2015**, *54*, 10429.
[33] W. H. Melhuish, *J. Phys. Chem.* **1961**, *65*, 229.

TOC Graphic